Computationally based explanation of the peculiar magneto-optical properties of PtMnSb and related ternary compounds

V. N. Antonov,* P. M. Oppeneer,† A. N. Yaresko,* A. Ya. Perlov,* and T. Kraft
Max-Planck Research Group ''Theory of Complex and Correlated Electron Systems,'' University of Technology, D-01062 Dresden, Germany
(Received 5 June 1997)

The magneto-optical (MO) spectra of 15 ternary ferromagnetic compounds are investigated on the basis of local-density band-structure calculations. The key material of interest in this study is PtMnSb, for which the MO Kerr spectra are unusually large and quite different from that of, e.g., the isoelectronic compounds NiMnSb and PdMnSb. First we show that the spectral differences between NiMnSb, PdMnSb, and PtMnSb can be fully understood from their relativistic electronic structure. Further, we investigate the following ternary ferromagnetic compounds: PtMnSn, PtCrSb, PtFeSb, Pt_2MnSb, Co_2HfSn, NiMnAs, PdMnAs, PtMnAs, RuMnAs, PtMnBi, BiMnPt, and PtGdBi. Within the total group of alloys, we study the MO spectra of PtMnSb in relationship to the spin-orbit coupling strength; the magnitude of the $3d$-magnetic moment; the degree of hybridization in the bonding; the half-metallic character, or, equivalently, the Fermi-level filling of the band structure; the intraband plasma frequency; and the influence of the crystal structure. We find that these characteristics form a unique combination in PtMnSb leading to its outstanding MO Kerr spectra. None of the other compounds can match up to PtMnSb in this respect. For the compounds NiMnAs, PdMnAs, PtMnAs, and, particularly, RuMnAs, whose MO spectra are not measured as yet, we predict Kerr spectra which look promising for ultraviolet laser light recording applications. [S0163-1829(97)01544-0]

I. INTRODUCTION

The Heusler alloys NiMnSb, PdMnSb, and PtMnSb have been the subject of intensive experimental and theoretical investigations since the early 1980s.[1–4] The interest in these compounds arose first from the experimental discovery of an extremely large magneto-optical (MO) Kerr rotation of $-1.27°$ in PtMnSb at room temperature.[1] This value was for many years the record Kerr rotation observed in a transition-metal compound at room temperature, and therefore called the ''giant'' Kerr effect (see, e.g., the recent surveys in Refs. 5 and 6). Almost simultaneously with the experimental discovery, the theoretical finding of the so-called ''half-metallic'' nature of PtMnSb was reported.[4] Half-metallicity means that, according to (semirelativistic) band-structure theory, the material is metallic for majority-spin electrons, but insulating for minority-spin electrons.[4] Such a gap for one spin type naturally may give rise to unusual magnetotransport and optical properties. The isoelectronic Heusler alloy NiMnSb also was predicted to be half-metallic, whereas the isoelectronic compound PdMnSb was predicted not to be half-metallic.[4] The MO Kerr rotations in both NiMnSb and PdMnSb, on the other hand, were experimentally found to be much smaller than that of PtMnSb, which resulted in a puzzling combination of features. Experimental efforts were undertaken to verify the proposed half-metallic character of NiMnSb and PtMnSb,[7–10] which was subsequently established in the case of NiMnSb.[7,10] Very recently, experimental evidence in favor of half-metallicity in PtMnSb was also reported.[11]

On the theoretical side, several model explanations of the MO spectra of the compounds were proposed.[12–14] One of these was based on a possible loss of the half-metallic character due to spin-orbit (SO) coupling, which was suggested to lead to a symmetry breaking between the different m states of the Sb p bands in the vicinity of the Fermi energy E_F.[12] Another explanation was based on differences of the semirelativistic effects in NiMnSb and PtMnSb,[14] and another one on enhancement of the MO Kerr spectra near the plasma resonance.[13] While the proposed models contain interesting physical mechanisms in themselves, one of the remaining major stumbling blocks was to explain the measured differences in the MO spectra of the isoelectronic NiMnSb, PdMnSb, and PtMnSb.

Owing only to the development of *ab initio* calculations of the MO spectra, a detailed quantitative comparison between experiment and first-principles spectra became feasible.[15–20] Heusler compounds are, of course, the most attractive materials for *ab initio* calculations of their MO spectra on account of the mentioned unusual features. Several first-principles calculations for these compounds were reported very recently.[21–25] The various calculated MO Kerr spectra, however, spread rather widely. The origin of the differences in the spectra obtained in the various calculations traces back, first, to the fact that the MO Kerr effect is a tiny quantity in calculations, related to the difference of reflection of left- and right-hand circularly polarized light.[6] SO coupling in the presence of spontaneous magnetization is responsible for symmetry breaking in the reflection of left- and right-hand circularly polarized light. Second, since the MO Kerr effect is only a tiny quantity in first-principles calculations, numerical accuracy and the influence of approximations made in the evaluation gain an appreciable importance. For this reason, the evaluation of the MO Kerr spectra of the ferromagnetic $3d$ transition metals Fe, Co, and Ni have become benchmark test cases for MO calculation

 © 1997 The American Physical Society

schemes.[15,16,19,20,26–29] Numerical accuracy normally does not play a decisive role if the physical mechanism is to be sought. However, is has been shown by several groups[16,19] that for the *ab initio* calculation of MO spectra an accurate evaluation of the dipole matrix elements is essential for obtaining numerically reliable MO Kerr spectra. Moreover, in the particular case of the Heusler alloys, the half-metallic band gap depends sensitively on technicalities of the band-structure calculation, as, e.g., atomic sphere radii.[24]

In the present work we report a detailed investigation of the MO Kerr spectra of NiMnSb, PdMnSb, and PtMnSb. In a recent survey of the current state of *ab initio* MO Kerr spectra calculations, the Kerr spectra we obtained for the three Heusler alloys were given,[25] but a full explanation of these Kerr spectra was not given (see also Ref. 30). In addition to examining these well-known compounds, we have investigated a group of 12 other ternary compounds, *viz*. PtMnSn, PtCrSb, PtFeSb, Pt_2MnSb, Co_2HfSn, NiMnAs, PdMnAs, PtMnAs, RuMnAs, PtMnBi, BiMnPt, and PtGdBi. These ternary compounds are related to PtMnSb, and can be derived from PtMnSb through selective chemical substitution (with the exception of Co_2HfSn). This study of the compounds derived by selective substitution can be viewed as a sort of ''materials engineering'' on the computer. The aim of investigating the whole group of compounds is twofold: First, it serves as an examination of the MO Kerr effect in PtMnSb on those quantities altered by substitution, as, e.g., SO coupling strength, half-metallicity, and magnetic moment. In the second place, the compounds are considered for their potential as MO storage material. In spite of the large Kerr rotation of PtMnSb, this material has, as a drawback for MO recording applications, a lack of a sufficient magnetocrystalline anisotropy which is required for a magnetic orientation perpendicular to the solids surface (see, e.g., Refs. 31 and 32). In this respect we mention that, in the last few years, promising materials for MO recording applications have been predicted on the basis of *ab initio* band-structure calculations.[33–35] The technologically motivated search, especially for suitable MO recording materials in the ultraviolet laser light range, is still continuing. For several of the compounds investigated here, we obtain, as will be discussed, promising MO Kerr spectra.

II. METHOD OF CALCULATION

The computational framework for the evaluation of the MO Kerr effect has been described previously in several papers.[16] We recall here that in the polar geometry, where the z axis is chosen to be perpendicular to the solids surface, and parallel to the magnetization direction, the Kerr effect is given by[36]

$$\theta_K(\omega)+i\varepsilon_K(\omega)=\frac{-\sigma_{xy}(\omega)}{\sigma_{xx}(\omega)\sqrt{1+\frac{4\pi i}{\omega}\sigma_{xx}(\omega)}}, \qquad (1)$$

with θ_K the Kerr rotation and ε_K the so-called Kerr ellipticity. $\sigma_{\alpha\beta}$ $(\alpha,\beta\equiv x,y,z)$ is the optical conductivity tensor, which is related to the dielectric tensor $\varepsilon_{\alpha\beta}$ through

$$\varepsilon_{\alpha\beta}(\omega)=\delta_{\alpha\beta}+\frac{4\pi i}{\omega}\sigma_{\alpha\beta}(\omega). \qquad (2)$$

The optical conductivity tensor, or equivalently, the dielectric tensor, is the important spectral quantity needed for the evaluation of the Kerr effect.[6] The optical conductivity can be computed from the energy band structure by means of the Kubo[37] linear-response expression:[38]

$$\sigma_{\alpha\beta}(\omega)=\frac{-ie^2}{m^2\hbar V_{uc}}\times\sum_{\mathbf{k}}\sum_{nn'}\frac{f(\epsilon_{n\mathbf{k}})-f(\epsilon_{n'\mathbf{k}})}{\omega_{nn'}(\mathbf{k})}\frac{\Pi^{\alpha}_{n'n}(\mathbf{k})\Pi^{\beta}_{nn'}(\mathbf{k})}{\omega-\omega_{nn'}(\mathbf{k})+i/\tau}, \qquad (3)$$

with $f(\epsilon_{n\mathbf{k}})$ the Fermi function, $\hbar\omega_{nn'}(\mathbf{k})\equiv\epsilon_{n\mathbf{k}}-\epsilon_{n'\mathbf{k}}$ the energy difference of the Kohn-Sham energies $\epsilon_{n\mathbf{k}}$, and $\gamma\equiv\tau^{-1}$ the lifetime parameter, which is included to describe the finite lifetime of excited Bloch electron states. Its physical effect is that each infinitely ''sharp'' optical transition is convoluted with a Lorentzian, of which γ is the half-width at half maximum. This lifetime parameter has originally been introduced on phenomenological grounds, but its appropriateness for describing the conductivity is beyond doubt.[38,16] $\Pi^{\alpha}_{nn'}$ are dipolar optical transition matrix elements, which in a fully relativistic description are given by

$$\mathbf{\Pi}_{nn'}(\mathbf{k})=m\langle\psi_{n\mathbf{k}}|c\boldsymbol{\alpha}|\psi_{n'\mathbf{k}}\rangle, \qquad (4)$$

with $\psi_{n\mathbf{k}}$ the four-component Bloch electron wave function. In the nonrelativistic limit, $\mathbf{\Pi}$ reduces to the canonical momentum $-i\hbar\nabla$.[39] $\psi_{n\mathbf{k}}$ and $\epsilon_{n\mathbf{k}}$ are calculated within the framework of the local-spin-density approximation (LSDA) to spin-density-functional theory.[40,41] To this end the Kohn-Sham-Dirac equation is solved (see, e.g., Refs. 42–46)

$$[c\boldsymbol{\alpha}\cdot p+\boldsymbol{\beta}mc^2+\mathbf{I}V+V_{\mathrm{sp}}\boldsymbol{\beta}\sigma_z]\psi_{n\mathbf{k}}=\epsilon_{n\mathbf{k}}\psi_{n\mathbf{k}} \qquad (5)$$

with $V_{\mathrm{sp}}(\mathbf{r})$ the spin-polarized part of the exchange-correlation potential corresponding to the z quantization axis. All other parts of the potential are contained in $V(\mathbf{r})$. The 4×4 matrices $\boldsymbol{\alpha}$, $\boldsymbol{\beta}$, and $\mathbf{I}$ are defined by

$$\boldsymbol{\alpha}=\begin{pmatrix}0 & \boldsymbol{\sigma}\\ \boldsymbol{\sigma} & 0\end{pmatrix},\quad \boldsymbol{\beta}=\begin{pmatrix}\mathbf{1} & 0\\ 0 & -\mathbf{1}\end{pmatrix},\quad \mathbf{I}=\begin{pmatrix}\mathbf{1} & 0\\ 0 & \mathbf{1}\end{pmatrix}, \qquad (6)$$

with $\boldsymbol{\sigma}$ the standard Dirac matrices, and $\mathbf{1}$ the 2×2 unit matrix. In the present work, Eq. (5) is solved self-consistently with a fully relativistic linear-muffin-tin-orbital method,[47,48] with variational inclusion of spin polarization.[46] For the LSDA exchange-correlation potential, the parametrization of von Barth and Hedin[49] has been used.

Expression (3) for the conductivity contains a double sum over all energy bands, which naturally separates in the so-called interband contribution, i.e., $n\neq n'$, and the intraband contribution $n=n'$. The intraband contribution to the diagonal components of $\boldsymbol{\sigma}$ may be rewritten for zero temperature as

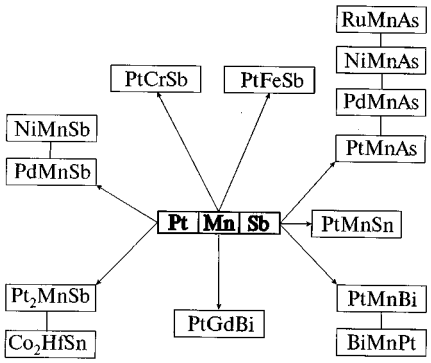

FIG. 1. The group of ternary intermetallic compounds which are investigated in relationship to the key compound, PtMnSb. The arrows indicate how the compounds are derived from PtMnSb through chemical substitution.

$$\sigma_{\alpha\alpha}(\omega) \equiv \frac{(\omega_{p,\alpha})^2}{4\pi} \frac{i}{\omega + i\gamma_D}, \tag{7}$$

with $\omega_{p,\alpha}$ the components of the plasma frequency, which are given by

$$(\omega_{p,\alpha})^2 \equiv \frac{4\pi e^2}{m^2 V_{uc}} \sum_{n\mathbf{k}} \delta(\epsilon_{n\mathbf{k}} - E_F) |\Pi^{\alpha}_{nn}|^2, \tag{8}$$

and E_F is the Fermi energy. For cubic symmetry, we furthermore have $\omega_p^2 \equiv \omega_{p,x}^2 = \omega_{p,y}^2 = \omega_{p,z}^2$. Equation (7) is identical to the classical Drude result for the ac conductivity, with $\gamma_D = 1/\tau_D$, and τ_D the phenomenological Drude electron relaxation time. The intraband relaxation time parameter γ_D may be different from the interband relaxation time parameter γ. The latter can be frequency dependent,[50] and, because excited states always have a finite lifetime, will be nonzero, whereas γ_D will approach zero for very pure materials. Here we adopt the perfect crystal approximation, i.e., $\gamma_D \rightarrow 0$. For the interband relaxation parameter, on the other hand, we shall use, unless stated otherwise, $\gamma = 0.03$ Ry. This value has been found to be, on average, a good estimate of this phenomenological parameter.[16]

We mention, finally, that the Kramers-Kronig transformation has been used to calculate the dispersive parts of the optical conductivity from the absorptive parts. The latter are obtained from a Brillouin-zone integral, which was performed using the tetrahedron technique.[51]

III. CALCULATED MO SPECTRA

The key material of interest in the present study is PtMnSb. In Fig. 1 we show schematically the group of ternary intermetallics related to PtMnSb that are investigated in the present study. The relationship of all of the displayed compounds to PtMnSb might not be obvious at first sight. The motivation is given in the following: The subgroup NiMnSb, PdMnSb, and PtMnsb constitute isoelectronic compounds, which exhibit the already mentioned unusual features. In PtCrSb and PtFeSb the magnetic element Mn has been substituted by Cr or Fe, its respective neighbors in the Periodic Table. Similarly, Sb has been substituted by Sn for PtMnSn. For PtMnBi, Sb has been replaced by Bi, which, again is an isoelectronic substitution. The effect of the atomic positions in the crystal structure is studied by interchanging, e.g., Pt and Bi, which yields BiMnPt. Other compounds which are isoelectronic with PtMnSb are given in the subgroup NiMnAs, PdMnAs, and PtMnAs. These compounds, interestingly, are known not to crystallize in the MgAgAs crystal structure, but in the hexagonal Fe_2P structure.[52] Also, RuMnAs crystallizes in the Fe_2P structure.[53] The inclusion of these compounds in the present study serves an illustration of the trends in the subgroup of the ternary arsenic intermetallics. In Pt_2MnSb the Pt content is doubled with respect to PtMnSb. The crystal structure changes correspondingly from the $C1_b$ half-Heusler structure, which has one empty site, to the so-called $L2_1$ crystal structure (cf. Ref. 3). Co_2HfSn also crystallizes in the $L2_1$ structure, and can be considered a reference compound with regard to its measured MO Kerr spectra.[3,5] PtGdBi, finally, serves to illustrate the impact of an enlargement of the magnetic moment due to replacement of Mn by Gd.

The lattice parameters which have been used in the calculations are the experimental ones.[52] In the few cases where the lattice parameter was not known, estimated values have been used.

A. PtMnSb, PdMnSb, and NiMnSb

One of the most surprising results reported for PtMnSb and NiMnSb is that band-structure calculations proposed these compounds to be half-metallic, but the isoelectronic compound PdMnSb was predicted not to be half-metallic.[4] The prediction of half-metallicity was based on semirelativistic band-structure calculations, i.e., the effect of SO coupling was neglected.[4] This approximation is often acceptable for the study of certain material properties, but especially for the investigation of MO properties it is not, because the Kerr effect is a purely relativistic effect. Recent *ab initio* relativistic calculations showed that the MO Kerr effect scales linearly with the SO coupling strength for monoatomic crystals.[54,55] The inclusion of SO interaction in the energy-band calculation could in principle destroy the half-metallic behavior, as was proposed in one model explanation of the MO Kerr spectra of PtMnSb.[12,5] In this model it is assumed that SO coupling lifts the degeneracy of the hybridized triplet Sb p band at the Γ point in such a way that the $m = +1$ level is raised above E_F, but the $m = 0$ and -1 levels fall below E_F.[12] If such a situation would actually happen, it would lead to an uncompensation of MO transitions stemming from $m = +1$ and -1 levels, which could be the reason for the large Kerr effect in PtMnSb.[12] However, in recent relativistic band-structure studies of PtMnSb, it was found that the half-metallic property nearly completely prevails,[56,24,57] and that therefore the supposed loss of half-metallicity due to SO coupling does not occur. To illustrate this relativistic band-structure result, in Fig. 2 we show the spin-projected, fully relativistic partial densities of states of PtMnSb. As can be recognized from Fig. 2, the partial densities of states for minority spin have evidently a gap at the Fermi level. We found a similar behavior for NiMnSb, but of course not for PdMnSb. For all three Heusler compounds we show, in Fig. 3, the calculated relativistic energy bands and total densities of state (DOS). In the case of PdMnSb, three spin-

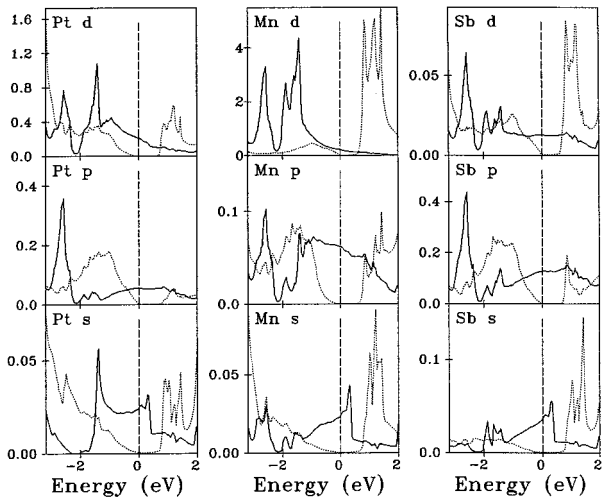

FIG. 2. Spin-projected, partial densities of state calculated for PtMnSb. Majority-spin densities are given by the full curves, minority-spin densities by the dotted curves. The half-metallic behavior can be seen from the band gap at the Fermi level, which is present for the minority spin, but not for the majority spin.

orbit-split energy bands are just above the Fermi level at the Γ-point, therefore half-metallic behavior is not supported for PdMnSb by band-structure theory. In the case of NiMnSb and PtMnSb, these important bands are just below E_F, rendering the half-metallicity in these compounds. Our band-structure results are in agreement with recent experiments on

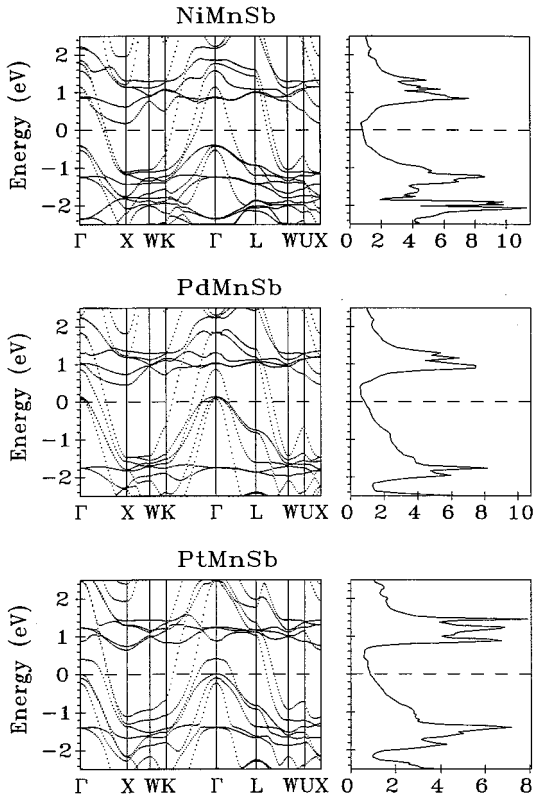

FIG. 3. Relativistic, spin-polarized energy-band structures and total densities of state (DOS) of NiMnSb, PdMnSb, and PtMnSb.

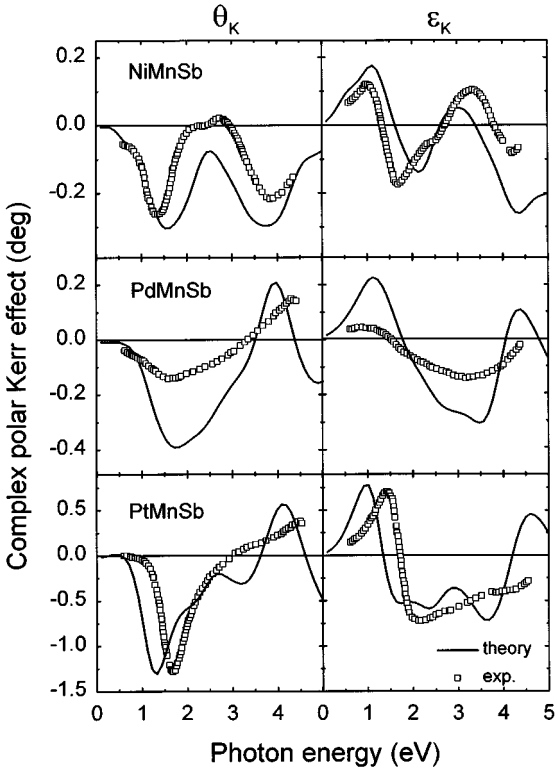

FIG. 4. Calculated and experimental Kerr rotation (θ_K) and Kerr ellipticity (ε_K) spectra of the Heusler compounds NiMnSb, PdMnSb, and PtMnSb. The experimental data are those of Refs. 1 and 3.

NiMnSb and PtMnSb, in which half-metallic behavior to a degree of nearly 100% was observed.[7,10,11]

After having verified the half-metallic band-structure property, we turn to the magneto-optical spectra. In Fig. 4 we show the calculated and experimental[1,3] MO Kerr spectra of the three isoelectronic Heusler compounds. There apparently exists a rather good agreement between the experimental Kerr spectra and the *ab initio* calculated ones. Overall, the experimental features are reasonably well reproduced, except for the magnitude of the Kerr rotation of PdMnSb, for which theory predicts larger values than are experimentally observed. The first and important conclusion, which we draw from the correspondence between experimental and calculated Kerr spectra, is: *the anomalous behavior of the MO Kerr spectra in these compounds is well described by normal band-structure theory*. While the calculated MO Kerr spectra of these three Heusler compounds were shown very recently in a review paper,[25] an explanation in detail of the origin of the depicted spectra was not yet given, which we will give in the following.

To investigate the origin of the Kerr spectra, we consider the separate contributions of both the numerator of Eq. (1), i.e., $\sigma_{xy}(\omega)$, and the denominator, $D(\omega) \equiv \sigma_{xx}[1 + (4\pi i/\omega)\sigma_{xx}]^{1/2}$. In Fig. 5 we show how the separate contributions of numerator and denominator bring about the Kerr angle of NiMnSb. The imaginary part of the inverse denominator (times the photon frequency), $\mathrm{Im}[\omega D]^{-1}$, displays a typical resonance structure at about 1 eV. The imaginary part of $\omega\sigma_{xy}$, i.e., $\omega\sigma_{xy}^{(2)}$, displays a double-peak structure. The double-peak structure of the Kerr rotation results

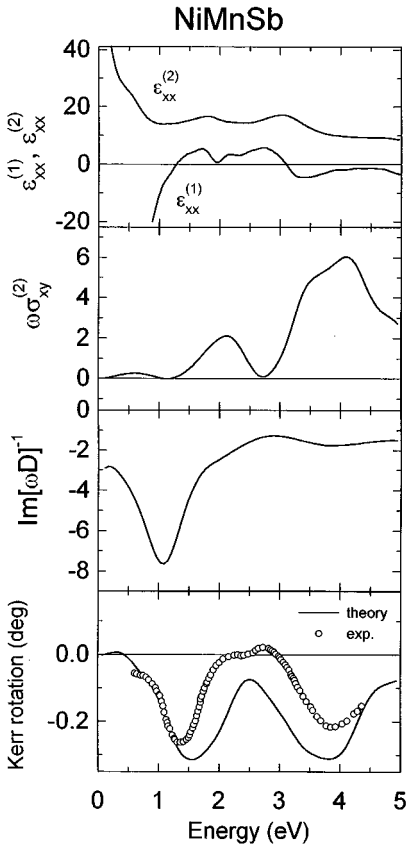

FIG. 5. Decomposition of the Kerr rotation spectrum of NiMnSb in separate contributions. Top panel: calculated real and imaginary part of the diagonal dielectric function, $\varepsilon_{xx}^{(1)}$ and $\varepsilon_{xx}^{(2)}$, respectively. Third panel from the top: The imaginary part of $[\omega D]^{-1}$ which results from $\varepsilon_{xx}^{(1)}$ and $\varepsilon_{xx}^{(2)}$. Bottom panel: The Kerr rotation which results as a combination of Im$[\omega D]^{-1}$ and $\omega\sigma_{xy}^{(2)}$ (second panel from the top). The experimental Kerr angle spectrum is after van Engen *et al.* (Ref. 1).

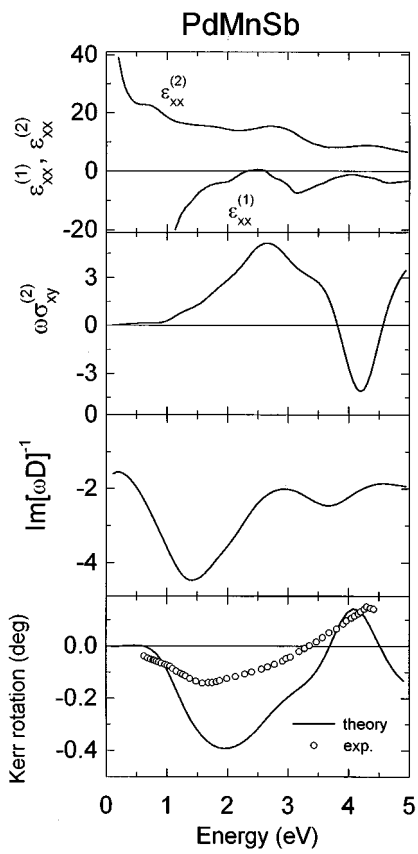

FIG. 6. As Fig. 5, but for PdMnSb.

roughly as the product of Im$[\omega D]^{-1}$ and $\omega\sigma_{xy}^{(2)}$: The first peak in the Kerr rotation at 1.5 eV is predominantly caused by a minimum of the denominator, whereas the second peak in the Kerr rotation at 4 eV is due to a maximum in the off-diagonal conductivity, $\omega\sigma_{xy}^{(2)}$. The nature of the peak in Im$[\omega D]^{-1}$ can be understand from the top panel in Fig. 5, where the complex diagonal dielectric function is shown: its real part, $\varepsilon_{xx}^{(1)}$, becomes small at about 1 eV, and its imaginary part $\varepsilon_{xx}^{(2)}$ has a shallow minimum at 1 eV. The second peak in the Kerr rotation stems from the maximum in $\omega\sigma_{xy}^{(2)}$, which in turn is known to be due to the interplay of SO coupling and spin polarization.[58,25] Thus the two similar-looking peaks in the Kerr rotation arise in fact from quite a different origin.

Next, we consider the spectra for the compound PdMnSb in more detail, which are shown in Fig. 6. In this compound $\omega\sigma_{xy}^{(2)}$ is larger than that of NiMnSb in the energy range 1–4 eV. This is simply due to the larger SO interaction on Pd as compared to that on Ni. The inverse denominator Im$[\omega D]^{-1}$, however, does not exhibit such a strong resonance as it does for NiMnSb. The latter is related to the particular shape of the $\varepsilon_{xx}^{(1)}$ and $\varepsilon_{xx}^{(2)}$ spectra. The Kerr rotation in effect displays the same shape as $\omega\sigma_{xy}^{(2)}$, being enhanced at 1–2 eV by the contribution from the denominator.

In Fig. 7 we show the spectral quantities for PtMnSb. The inverse denominator Im$[\omega D]^{-1}$ again displays for PtMnSb a strong resonance at 1 eV, which is even larger than that for NiMnSb. In addition, the off-diagonal conductivity $\omega\sigma_{xy}^{(2)}$ is for PtMnSb again larger than that of PdMnSb, in accordance with the larger SO coupling on Pt. The resulting Kerr rotation has a ''giant'' peak of $-1.2°$ up to $-2.0°$ depending on the applied lifetime parameter (see Fig. 7). These values are in good agreement with the available experimental Kerr peak values for PtMnSb, which range from about $-1°$ to $-2°$ depending on sample preparation and surface quality.[1,31,32,59–65] Careful investigations of the consequences of sample preparation were performed by Takanashi *et al.*[60] and Sato and co-workers.[64,65] These investigations showed that annealing of the PtMnSb sample raises the Kerr angle to a maximum value of $-2°$, whereas the nonannealed Kerr angle is only $-1.2°$. The off-diagonal conductivity $\omega\sigma_{xy}^{(2)}$ was found to be rather insensitive to annealing (see Fig. 7).[64,65] The main impact of annealing thus evidently occurs in the denominator. The reason for the calculated resonance in the inverse denominator lies again in the frequency dependence of the diagonal dielectric function, which is shown in the top panel of Fig. 7. The calculated ε_{xx} compares reasonably well with the experimental one,[65] except for the important first root frequency of $\varepsilon_{xx}^{(1)}$ which is shifted by about 0.5 eV. This difference leads to a shifted position in the resonance peak of Im$[\omega D]^{-1}$, which in turn results in a shifted main Kerr rotation peak of just the same amount. The

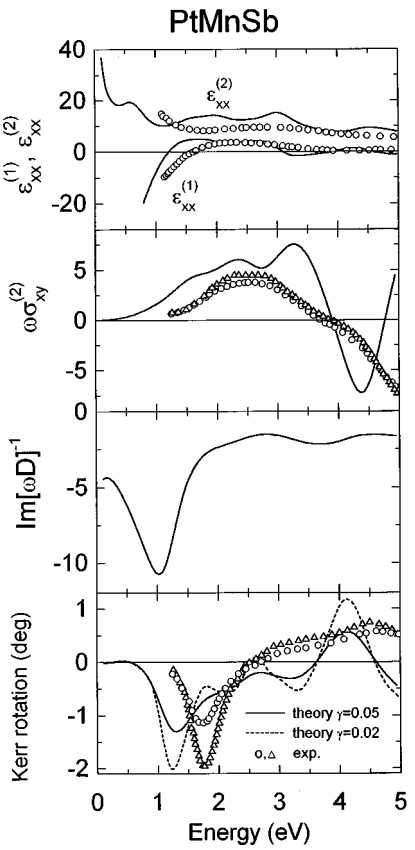

FIG. 7. As Fig. 5, but for PtMnSb. The experimental data are after Ikekame *et al.* (Ref. 65). The data for annealed PtMnSb are denoted by △, and those for nonannealed, polished PtMnSb by ○. The calculated Kerr rotation spectrum is shown for two interband lifetime parameters, $\gamma=0.05$ and $\gamma=0.02$ Ry.

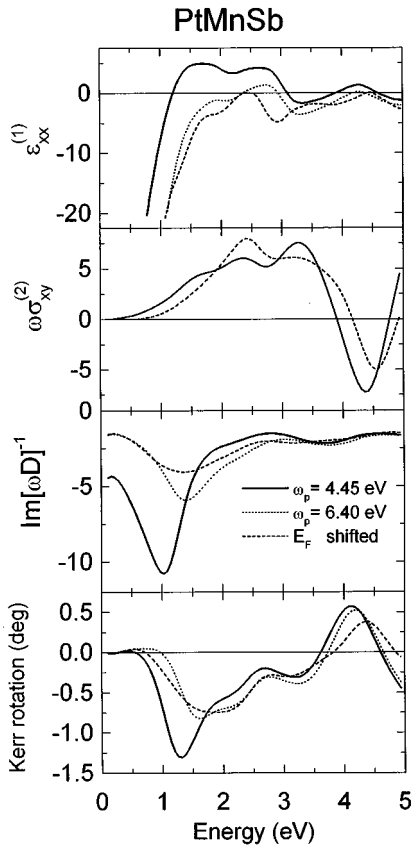

FIG. 8. Model investigation of the influence of the half-metallic character of PtMnSb on the optical and MO spectra. A non-half-metallic band structure has been modeled in two ways: by artificially shifting E_F in PtMnSb down, and by increasing the calculated plasma frequency $\omega_p=4.45$ eV to 6.40 eV.

position of the maximum in $\mathrm{Im}[\omega D]^{-1}$ thus predominantly determines the position of the main Kerr rotation peak. We mention, in addition, that the second maximum in the calculated $\omega\sigma_{xy}^{(2)}$ at 4.4 eV (see Fig. 7) is also present in the experimental spectrum, but at a higher energy of 5.2 eV.[65]

The origin of the giant Kerr angle in PtMnSb, as compared to the Kerr angles in NiMnSb and PdMnSb, can completely be understood from our calculations. In these three compounds, first, the off-diagonal conductivities $\sigma_{xy}(\omega)$ are quite different, which is a direct result of the different relativistic electronic structure. Although both NiMnSb and PtMnSb are both half-metallic, their $\omega\sigma_{xy}^{(2)}$ spectra are distinctly different, while on the other hand the $\omega\sigma_{xy}^{(2)}$ of PdMnSb and PtMnsb have a similar structure, but not a similar magnitude (see Figs. 5, 6, and 7). In the second place, there is the influence of the denominators, as exemplified in Im $[\omega D]^{-1}$. These are similar in shape and magnitude for NiMnSb and PtMnSb, but the magnitude of $\mathrm{Im}[\omega D]^{-1}$ in PdMnSb is about a factor of 2 smaller. We find that this difference relates to the half-metallic nature of both NiMnSb and PtMnSb, which is not present for PdMnSb. From Fig. 3 it can be seen that for the half-metallic compounds there are three lesser bands at E_F. One consequence is therefore that the intraband contribution to σ_{xx} will be smaller [see Eq. (8)]. In Fig. 8 we show the impact of the half-metallic character of the band structure on the Kerr rotation of PtMnSb. The calculated plasma frequency in PtMnSb is small, $\hbar\omega_p=4.45$ eV. Experimentally a somewhat larger plasma frequency of (6.1 ± 0.4) eV was found for PtMnSb, and a smaller $\hbar\omega_p=(4.9\pm0.2)$ eV for NiMnSb.[66] One should, however, not forget that the sample purity can affect the plasma frequency through the position of E_F. To investigate the influence of the half-metallicity, we can artificially shift the Fermi energy down, and calculate the spectra for this position of E_F, or we can leave E_F as it is, and model a non-half-metallic band structure by adopting a larger ω_p. Both ways to mimic non-half-metallicity have a drastic impact on the resulting Kerr rotation, which becomes reduced by a factor 2. As can be seen from the top panel in Fig. 8, in the absence of half-metallicity the shape of $\varepsilon_{xx}^{(1)}$ changes, and closely resembles that of PdMnSb (see Fig. 6). This is especially so for the model where E_F is shifted, since this leads to the smaller $\mathrm{Im}[\omega D]^{-1}$, and also to a reduction of $\omega\sigma_{xy}^{(2)}$ at photon energies below 2 eV. The latter is due to the exclusion of optical transitions from the SO-split bands just below E_F. The consequence of both models for non-half-metallic behavior is that the maximum in $\mathrm{Im}[\omega D]^{-1}$ becomes about two times smaller. The Kerr angles derived in these models resemble now that of PdMnSb in shape, but are larger, because $\omega\sigma_{xy}^{(2)}$ is larger than that of PdMnSb. Previously, we showed that if the SO coupling on Pt in PtMnSb is artificially set to zero, the Kerr rotation peak in PtMnSb becomes re-

duced by a factor of 3.[24] We mention, with respect to the influence of the denominator on the Kerr rotation in PtMnSb, that experiments in which the stoichiometry and crystalline sample quality were varied also concluded that the denominator contributed appreciably to the giant Kerr rotation.[60,62–65]

In conclusion, we find that the Kerr spectra of NiMnSb, PdMnSb, and PtMnSb can be fully understood from their electronic structure. The puzzling anomalities in the Kerr spectra of these compounds arise from an interplay of compound related differences in the SO interaction, in the half-metallic character, and also in relative positions of energy bands.

Previously, several model explanations for the giant Kerr effect in PtMnSb were proposed.[12–14] We already discussed the model which assumed the destruction of half-metallicity caused by SO coupling.[12] Another model suggested that scalar-relativistic effects and not the SO interaction are responsible for the differences in the Kerr spectra of the three Heusler compounds.[14] However, as we already emphasized, the SO interaction largely determines the Kerr spectra in these intermetallic compounds. The explanation proposed by Feil and Haas[13] is based on the assumption that at $\varepsilon_{xx}^{(1)}=1$ a resonance in the inverse denominator D^{-1} occurs, and that σ_{xy} plays no role. We do find that an important resonance in the denominator occurs, though not necessarily precisely at those energies where $\varepsilon_{xx}^{(1)}=1$ (see also Ref. 67). For example, in the case of NiMnSb and PtMnSb there are two energies where $\varepsilon_{xx}^{(1)}=1$. In addition, as we showed above, σ_{xy} does as much play a role in the giant Kerr rotation as the denominator does. Attention to the enhancing effect that a small denominator has on the Kerr rotation was drawn previously for TmS and TmSe,[68] and very recently for CeSb, for which compound a record Kerr rotation of 90° was detected.[69,70]

Recently, two other *ab initio* calculations of the Kerr spectra of these Heusler compounds were reported.[21–23] In the study of Ref. 22, the correct experimental magnitude of the Kerr rotation in NiMnSb was obtained, but the large Kerr rotation in PtMnSb could not be reproduced. Conversely, in another study by Kulatov and co-workers[22,23] a large Kerr rotation was obtained for PtMnSb; however, for NiMnSb, a theoretical Kerr rotation three times larger than the experimental one was calculated. Undoubtedly, this unusually wide spread in the *ab initio* calculated Kerr spectra reflects the major influence of numerical accuracy in the calculations. With regard to the wide spread in the theoretical Kerr rotations we mention that we very recently predicted for $CrPt_3$ and $MnPt_3$ large Kerr rotations with peak (interband) values of $-0.9°$ and $-1.5°$, respectively,[35] in reasonable agreement with existing experiments for $MnPt_3$.[71,72] Yet another first principles calculation by Kulatov, Uspenskii, and Halilov[73] gave much larger Kerr rotations of even $-2.1°$ and $-2.5°$ for $CrPt_3$ and $MnPt_3$. Notably, apart from the magnitude of the MO Kerr peaks, the later calculation also predicts a different trend with respect to the $3d$ element. However, the trend and shape of the Kerr spectra we predicted for $CrPt_3$ and $MnPt_3$ was very recently confirmed experimentally by Vergöhl and Schoenes.[74] Particular for the Heusler compounds, computational accuracy is imperative, in view of the conclusions concerning the physical mechanism that are to be derived. As documented by our previous experience in computing MO spectra, we believe that we have taken sufficient care to obtain trustworthy first-principles spectra.[16,20,24,75]

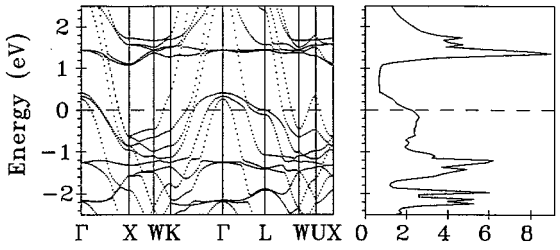

FIG. 9. Fully relativistic, spin-polarized energy band structure and density of states (DOS) of PtMnSn.

B. PtMnSn

One of the compounds that, from the beginning of the discovery of the anomalous properties of MnPtSb, has been considered in relationship to PtMnSb is PtMnSn.[1,4,76,77] Although Sb and Sn are neighbors in the Periodic Table, the MO Kerr rotation in PtMnSn was measured to be much smaller than that of PtMnSb.[2] Scalar-relativistic band-structure calculations predicted that PtMnSn is not half-metallic.[4,76] We performed fully relativistic band-structure calculations which lead to the same conclusion; see Fig. 9. If one were to fill the energy bands of PtMnSn with one more electron, a half-metallic band structure comparable to that of PtMnSb (see Fig. 3) would result. For this reason, we expect the MO Kerr spectra of PtMnSn to be similar to those calculated for PtMnSb with a down-shifted E_F. In Fig. 10 we show the theoretical and experimental Kerr spectra for PtMnSn. The calculated Kerr rotation and ellipticity curves of PtMnSn resemble the shape of the experimental curves, but the theoretical size of the spectra is much larger. At present, we do not know what the reason is for this unusual discrepancy between LSDA energy-band theory and

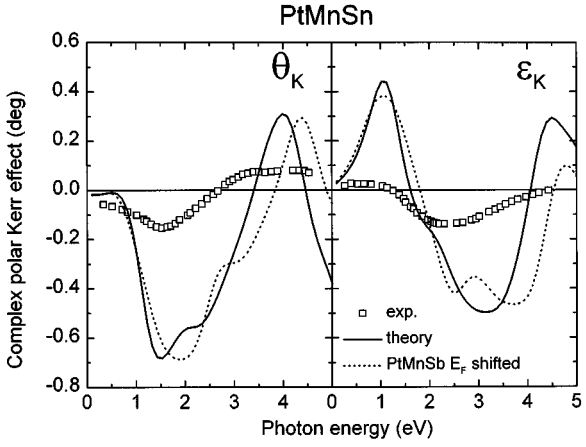

FIG. 10. Calculated theoretical and experimental (Ref. 1) Kerr angle (θ_K) and Kerr ellipticity (ε_K) of PtMnSn. For comparison, the Kerr spectra that result for PtMnSb when the Fermi level is artificially shifted down are also shown (dashed curves).

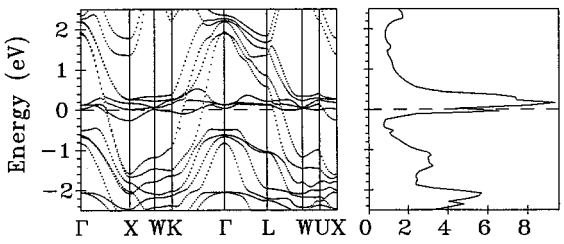

FIG. 11. Fully relativistic, spin-polarized energy band structure and DOS of PtFeSb in the $C1_b$ half-Heusler crystal structure.

experiment. One possible explanation, which is as yet purely speculative, is that it could be that the PtMnSn sample had a poor crystalline quality. Poor crystalline ordering of a sample has previously been shown to reduce the magnitude of the Kerr effect.[34,78] In Fig. 9 we also show the effect of a down-shifted Fermi level on the MO Kerr spectra of PtMnSb. As anticipated, these spectra closely correspond to the *ab initio* calculated spectra of PtMnSn. We can therefore safely conclude that the main reason for the differences in the Kerr effect in these two compounds is the critical position of the Fermi level.

C. PtCrSb and PtFeSb

Cr and Fe are the respective neighbors of Mn in the Periodic Table. Both the ternary alloys PtCrSb and PtFeSb were studied previously in connection to PtMnSb.[79] It came as a surprise when it was found that PtCrSb and PtFeSb do not crystallize in the half-Heusler crystal structure, but in a closely related structure, in which the Sb and Cr (or Fe) atoms have shifted somewhat from the ideal positions.[79] Moreover, it was found that in PtFeSb, Fe carries a large magnetic moment of 2.5 μ_B, but PtCrSb was found to be nonmagnetic.[79] In addition, the Kerr spectra of PtFeSb were measured to be totally different from those of PtMnSb: The maximal Kerr rotation in PtFeSb was about 20 times smaller than that of PtMnSb.

With the aim of understanding the microscopic reason for this unusual materials dependence, we performed calculations for PtFeSb and PtCrSb in their distorted Heusler structures, but for comparison we also calculated PtFeSb, assuming an ideal half-Heusler structure. In Fig. 11 we show the relativistic band structure of PtFeSb assuming an ideal $C1_b$ structure. In this structure, there is, for PtFeSb, a quasigap at about 0.4 eV below E_F. A closer inspection of the spin-projected DOS has revealed that at this energy the band structure is half-metallic. Thus PtFeSb can in a simplified picture be considered as an analog of PtMnSb, in which the bands are filled with one more electron. In Fig. 12 we depict the experimental and theoretical MO Kerr spectra of PtFeSb. The theoretical spectra are shown for three cases: the distorted half-Heusler crystal structure, the ideal $C1_b$ half-Heusler structure, and the ideal $C1_b$ structure, but with E_F shifted such that the material would be half-metallic. We find that for the half-Heusler structure LSDA band structure theory predicts for PtFeSb a reasonable maximum Kerr rotation of about $-0.4°$. If the Fermi level is shifted, however, so that the material artificially becomes half-metallic, the Kerr angle peak is predicted to be enhanced to nearly

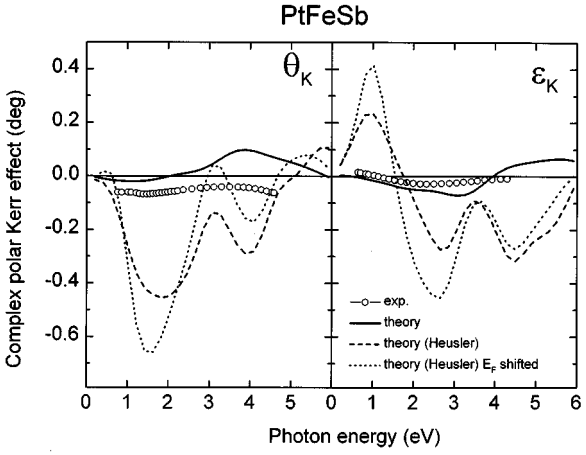

FIG. 12. Theoretical and experimental (Ref. 79) results for the polar Kerr spectra of PtFeSb. The theoretical Kerr spectra are given for two crystal structures: the distorted $C1_b$ crystal structure, which is the experimentally observed structure (solid curves), and the ideal $C1_b$ half-Heusler structure (dashed curves). For the latter structure, the influence of a shift of the Fermi level into the spin minority-band gap, making the band structure half-metallic, is also shown.

$-0.7°$. The mechanism for this enhancement is of course just the same as what we explained for PtMnSb. Noticeably, we recognize from Fig. 12 that the crystal structure has an enormous impact on the Kerr spectra: the calculated Kerr spectra for the true crystal structure are much smaller than obtained for the $C1_b$ structure. The *ab initio* calculated Kerr rotation and Kerr ellipticity are in shape and magnitude in good agreement with the experimental data.[79] Thus our first-principles calculations fully support the previously as unusual considered differences between the MO Kerr spectra of PtFeSb and PtMnSb. The reason for the enormous difference between the calculated Kerr spectra of PtFeSb in the two structures is the difference in the corresponding electronic structures. In Fig. 13 the relativistic band structure and DOS of PtFeSb in the distorted half-Heusler structure is shown. It is certainly not possible to understand solely from the band structures why one compound has a small Kerr angle while another one has a large Kerr angle. To illustrate the origin of the different Kerr spectra, in Fig. 14 we show the absorptive components of σ_{xx} and σ_{xy}. In the case of PtFeSb, all allowed interband contributions of all bands cooperate in such a way that these nearly cancel for $\sigma_{xy}^{(2)}(\omega)$ in the distorted Heusler phase. The diagonal conductivity $\sigma_{xx}^{(1)}(\omega)$, on the

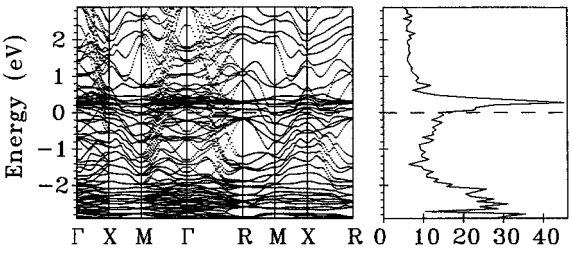

FIG. 13. Relativistic energy bands and DOS (right-hand panel) of PtFeSb in the distorted half-Heusler structure (space group No. 198).

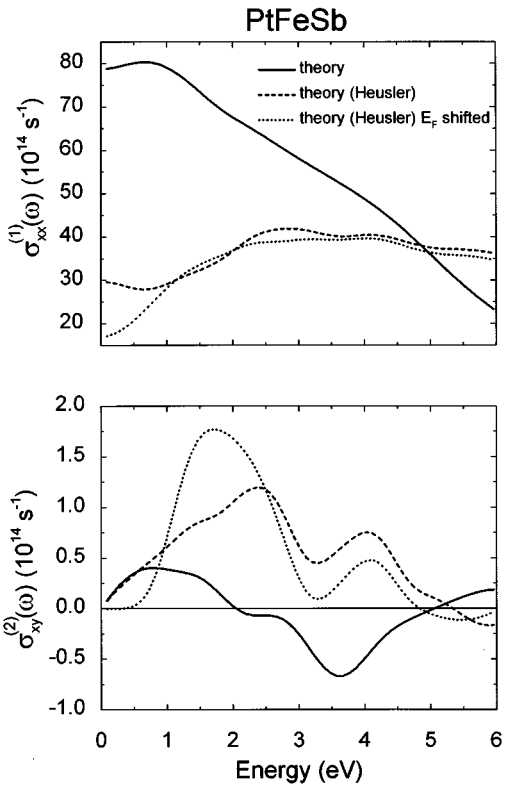

FIG. 14. Calculated absorptive parts of the optical conductivity, $\sigma_{xx}^{(1)}$ and $\sigma_{xy}^{(2)}$, for PtFeSb in two different crystal structures (see text).

other hand, is additive in the allowed interband optical transitions, and is therefore much larger in the distorted phase than it is in the ideal $C1_b$ phase. The combination of a relatively small off-diagonal conductivity and a large diagonal conductivity brings about a small Kerr effect in PtFeSb.

The related ternary compound PtCrSb also crystallizes in the distorted half-Heusler structure. This compound does not order magnetically.[79] To study the influence of the Cr substitution on the MO Kerr spectra, we performed *ab initio* calculations for PtCrSb using constraint LSDA calculations to obtain a ferromagnetic solution. The thus-calculated Kerr spectra are given in Fig. 15. LSDA energy-band theory predicts a rather small Kerr effect in PtCrSb, which is nevertheless about two times larger than the Kerr effect in PtFeSb. This again is an electronic structure effect. We do not show the energy-band structure of PtCrSb here, but mention that the positions of the energy bands with respect to E_F are different from those in PtFeSb (Fig. 13), for which reason the contributions to $\sigma_{xy}^{(2)}$ do not cancel as much. The diagonal conductivity $\sigma_{xx}^{(1)}$, however, is almost the same in PtFeSb and in PtCrSb. In comparison to PtMnSb, the substitution of Fe or Cr for Mn is thus not favorable for the MO properties. We find that this is primarily an effect of the concomitant lattice structure changes.

D. Pt_2MnSb and Co_2HfSn

The $C1_b$ half-Heusler structure contains one empty lattice site (see, e.g., Ref. 3). If this lattice site in the formula composition XYZ is filled with one X atom, the $L2_1$ structure for

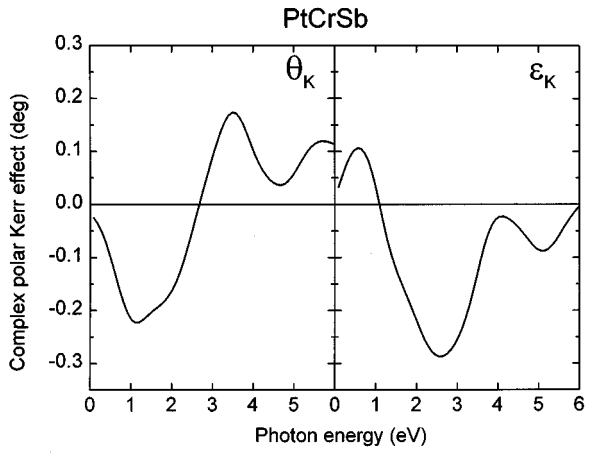

FIG. 15. Theoretical Kerr angle and Kerr ellipticity of PtCrSb in the distorted half-Heusler structure.

the X_2YZ composition arises. The compound Pt_2MnSb is therefore in this sense the $L2_1$ extension of PtMnSb. It would be interesting to examine the MO properties of Pt_2MnSb in comparison to those of PtMnSb, yet to our knowledge it appears that this has not been done experimentally. In several previous theoretical studies, it was demonstrated that when the strength of the SO interaction is increased in a ferromagnetic material, the Kerr effect will in general become larger.[16,24,35] One possible means of increasing SO coupling is of course by substitution of, or alloying with, heavy elements, as, e.g., Pt or Bi. The Kerr effect in FePt will consequently be larger than that in FePd, which is in turn larger than that in Fe.[33] One might on these arguments expect a larger Kerr effect in Pt_2MnSb than in PtMnSb, if one of course would forget for a moment that PtMnSb does not at all exhibit a standard behavior. In addition to the SO coupling, also the local symmetry of Pt atoms around one Mn atom is different: For the $L2_1$ crystal structure the local symmetry around the Mn site is cubic, whereas for the $C1_b$ crystal structure it is trigonal.

In Fig. 16 we show the calculated Kerr spectra of Pt_2MnSb. For comparison, we also give calculated spectra for Co_2HfSn, because for this compound experimental spec-

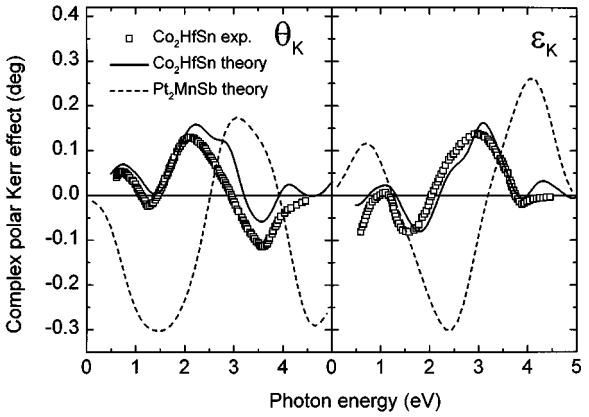

FIG. 16. Kerr rotation and Kerr ellipticity of the Heusler alloys Pt_2MnSb and Co_2HfSn. The experimental Kerr spectra of Co_2HfSn are after Ref. 2.

tra were measured.[2,3] In spite of the SO coupling, which is added through the extra Pt atom, the Kerr effect in Pt_2MnSb is calculated to be much smaller than that in PtMnSb. From the comparison between the experimental and calculated Kerr spectra of Co_2HfSn, we conclude that the theoretical description of this compound is quite good, which we would thus anticipate also to hold for Pt_2MnSb. The reason that the Kerr effect in Pt_2MnSb is much smaller than that in PtMnSb again follows from the band structures. The band structure of Pt_2MnSb, which we do not show here, is quite different from that of PtMnSb, and, moreover, not half-metallic. The Kerr effect in Pt_2MnSb is also small compared to that of $MnPt_3$, where a maximum interband Kerr angle of $-1.5°$ was calculated.[24,35] In Pt_2MnSb the interband transitions contributing to σ_{xy} cancel to a large extent each other, as a particular consequence of the electronic structure.

E. PtMnBi, BiMnPt, and PtGdBi

The basic idea behind the investigation of PtMnBi and BiMnPt is similar to that of Pt_2MnSb, namely, to try to enlarge the SO coupling strength within the hybridized bands by substitution of a heavier element. An isoelectronic substitution in this manner is PtMnBi. Previously it was shown in *ab initio* calculations that MnBi has a larger Kerr rotation than MnSb, because of the larger SO coupling of Bi.[75] In PtMnBi the Mn atom has Pt nearest neighbors. There is thus the largest overlap between Pt and Mn orbitals. In MnBi, which also is experimentally known to exhibit a giant Kerr angle up to $-2°$,[80,81] the Mn d orbitals overlap with Bi p orbitals. Therefore it is also of interest to consider BiMnPt, i.e., Bi and Pt atoms interchanged. We note, however, that the Kerr spectra of PtMnBi and BiMnPt have not been measured, perhaps these compounds do not even exist in this crystal structure. An earlier theoretical study examined both NiMnSb and MnNiSb in this respect, in order to determine the ground-state energy composition,[82] but this is not our present aim. The third compound, PtGdBi, does exist in the $C1_b$ crystal structure,[83,84] but MO measurements were not undertaken for this compound. In PtGdBi the Gd atom is expected to carry a much larger magnetic moment than that of Mn. A larger moment leads often to a larger Kerr rotation.[25,35]

The theoretical Kerr spectra of these three compounds are given in Fig. 17. Let us first consider PtMnBi in comparison to PtMnSb. We find for PtMnBi a maximal Kerr rotation of $-0.7°$, which is much smaller than the one calculated for PtMnSb. The band structure of PtMnBi, which is shown in Fig. 18, gives us the information that PtMnBi, in contrast to PtMnSb, is not half-metallic. At 0.2 eV above E_F there is a small gap visible at the Γ point. With the Fermi level at this energy position, the band structure would be half-metallic. However, compared to PtMnSb there are further differences: at the Γ point, the triplet bands and the singlet levels, which are of mixed Pt and Mn s character, hybridize in a different manner from the equivalent bands in PtMnSb (see, e.g., Ref. 12). The consequence is that the optical conductivities, and thus the Kerr spectra, differ from those of PtMnSb. The Kerr effect in BiMnPt is, for photon energies up to 3–4 eV, similar to that in PtMnBi. The Mn d states overlap in BiMnPt mainly with Bi p states, yet, due to the large exchange splitting of nearly 3 eV in the Mn $3d$ bands, the energy bands of BiMnPt are, close to the Fermi level, comparable to those of PtMnBi.

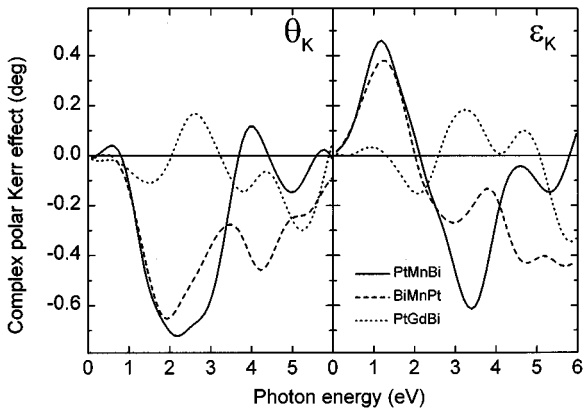

FIG. 17. Theoretical Kerr angle θ_K and Kerr ellipticity ε_K of PtMnBi, BiMnPt, and PtGdBi.

The calculated Kerr effect in PtGdBi shows a spectral dependence which is rather different from that of PtMnBi and BiMnPt (see Fig. 17). Compared to PtMnBi, the absolute size of the Kerr angle in PtGdBi is particularly small. With respect to our calculations for this compound, we should mention that it is still being discussed in the literature if LSDA band structure theory can properly describe pure Gd (see, e.g., Refs. 85 and 86). Such doubts could be equally valid for Gd compounds, but for the present consideration we shall ignore these doubts. We calculate the LSDA exchange splitting of Gd in PtGdBi to be about 5 eV, which is thus larger than that of Mn. The spin-polarized, relativistic energy bands and DOS of PtGdBi are shown in Fig. 19. Although the exchange splitting on Gd is large, this does not give rise to a large Kerr effect. The reason for this lies in the fact that the rather localized Gd $4f$ bands do not hybridize so much with the Bi p and Pt d bands. In Fig. 20 the partial DOS's of PtGdBi are depicted. In contrast to the partial DOS's of PtMnSb, which are shown in Fig. 2, the Pt and Bi bands in PtGdBi do nearly not spin polarize, as a result of the small hybridization with the Gd $4f$ bands, in spite of the large moment being present on the Gd site. Therefore the contributions of the optical transitions, for the two spin directions that take place within the hybridized Pt and Bi bands, cancel each other to a large extent, and a small σ_{xy} is the consequence. We remark furthermore that our calculations predict PtGdBi to be a narrow-gap semiconductor, in

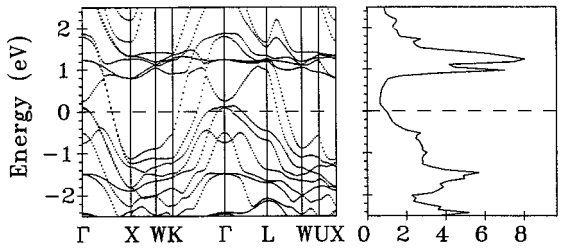

FIG. 18. Spin-polarized, relativistic energy bands and total DOS of PtMnBi.

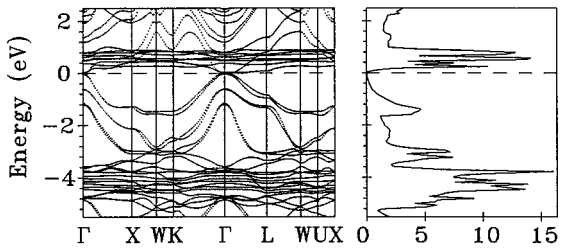

FIG. 19. As Fig. 18, but for PtGdBi. Note the narrow gap at the Fermi energy.

agreement with experiment.[83] This property we obtain in the *ferromagnetic* phase of PtGdBi, which thus would place PtGdBi theoretically in the exceptional group of ferromagnetic semiconductors, to which belong, for instance, $CrBr_3$, CrI_3, EuO, and EuS (see, e.g., Refs. 87–89). Experimental investigations do, however, show that most likely antiferromagnetic, instead of ferromagnetic, ordering takes place in PtGdBi.[83] Our calculations for the MO Kerr spectra of PtGdBi would then correspond to PtGdBi in an applied magnetic field.

F. NiMnAs, PdMnAs, PtMnAs, and RuMnAs

Next we consider the related group of ternary compounds NiMnAs, PdMnAs, and PtMnAs, as well as RuMnAs. Similar to the isoelectronic substitution of Bi for Sb, investigated in Sec. III E, we can substitute As for Sb. This substitution thereby leads to a reduced SO coupling strength of As as compared to that of Sb. At first sight the isoelectronic substitution of As might seem straightforward, however; it has been discovered experimentally that with As instead of Sb, NiMnAs and PdMnAs do not crystallize in the MgAgAs crystal structure, but in the hexagonal Fe_2P structure.[90–92] The compound PtMnAs has, to our knowledge, not been investigated experimentally. For this compound we shall assume a Fe_2P crystal structure also.

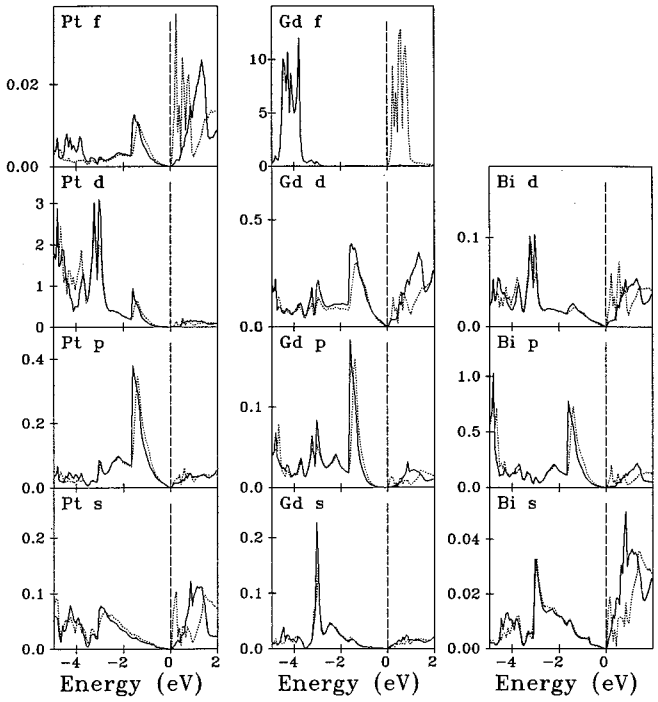

FIG. 20. Spin-projected partial DOS's of PtGdBi. Majority-spin densities are given by the full curve, minority-spin densities by the dotted curves.

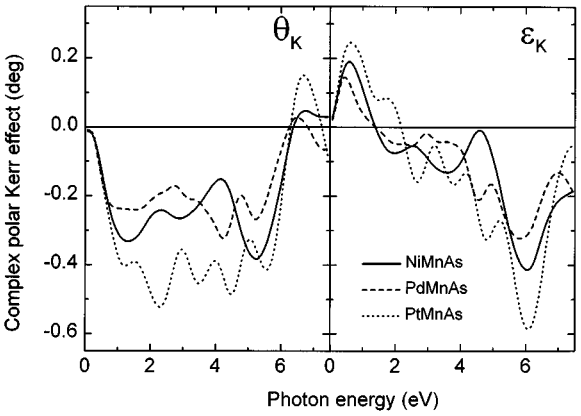

FIG. 21. Theoretical Kerr rotation and Kerr ellipticity spectra of the ternary alloys NiMnAs, PdMnAs, and PtMnAs in the Fe_2P crystal structure.

The MO Kerr spectra of these ternary arsenic compounds have not been measured as yet. In Fig. 21 we present their *ab initio* calculated Kerr spectra. The Kerr rotations are for these compounds calculated to be relatively small, of about $-0.2°$ to $-0.5°$ maximally. Apart from the smaller SO coupling of As, of course the crystal structure different from the $C1_b$ structure comes into play. Hence the shape of the Kerr rotation spectra bears no direct correspondence to that of the Sb-based half-Heusler alloys. For the sake of completeness, we show the band structures and total DOS's of the three As-based compounds in Fig. 22. Just like the ternary Sb-

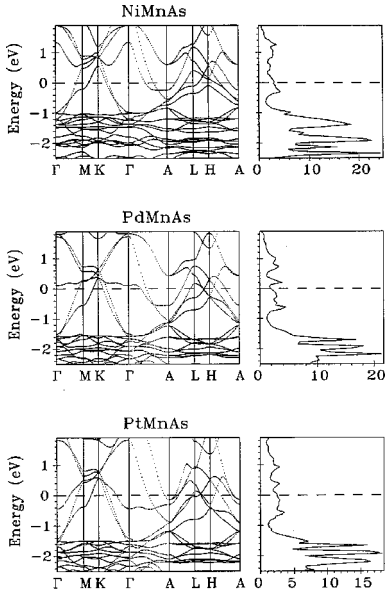

FIG. 22. Relativistic band structures and total DOS's of NiMnAs, PdMnAs, and PtMnAs.

compounds, the related As-compounds are found to have a low DOS at E_F, which are formed predominantly of hybridized As p bands.

The three Fe_2P structure compounds are not calculated to exhibit large Kerr effects. Nevertheless, these compounds could be attractive for MO recording applications. One of the reasons for this is that the magnetic anisotropy in the hexagonal Fe_2P phase is in general much larger than that of the cubic $C1_b$ compounds. In cubic compounds the magnetic anisotropy energy scales approximately with the fourth power of the SO coupling strength, whereas in a hexagonal or uniaxial symmetry it scales as the square of the SO coupling.[93–95] Therefore either uniaxial multilayered or hexagonal materials are more favorable for MO recording applications, since such materials exhibit the sufficiently large magnetic anisotropy which is required to sustain the local magnetization orientation perpendicular to the MO disk surface.[5,96–98] In addition to the cubic structure, PtMnSb has for MO recording applications the drawback that, at the photon frequency where the peak Kerr rotation occurs, the reflectivity becomes small.[63–65] This is of relevance for the so-called figure of merit, which is proportional to the signal-to-noise ratio in MO reading, and which is therefore used as a measure for the MO recording quality of a material.[6,96] The figure of merit is commonly defined as $R^{1/2}(\theta_K^2+\varepsilon_K^2)^{1/2}$, with R the reflectivity, which can directly be computed from the optical conductivity.[6,36] In the case of PtMnSb the small reflectivity therefore partially compensates for the advantage of the giant Kerr rotation at 1.7 eV. A third drawback that PtMnSb has, particularly for modern MO recording applications, is the energy position of the peak rotation. Future second-generation high-density MO storage devices will utilize ultraviolet lasers, i.e., have photon energies of about 3–4 eV.[78]

In comparison to PtMnSb, As-based ternary intermetallics do have the following advantages for MO recording applications: a reasonable Kerr effect at 3–4 eV, a normal metallic reflectivity, and, expectantly, a sufficiently large magnetocrystalline anisotropy. The physical properties of these compounds have been poorly investigated. It is therefore unclear at present if they exhibit certain disadvantages for applications in MO devices. In the case of PdMnAs it is known that the Curie temperature is about 200 K,[92] which thus excludes this compound for room temperature MO applications.

The question thus remains if we can identify compounds which could be suitable MO recording materials. Within the group of MnAs-based compounds, it has previously been found that RuMnAs crystallizes in the Fe_2P structure,[53] and is ferromagnetic with $T_C=497$ K.[92] In contrast to PdMnAs, this T_C is appropriate for thermomagnetic writing.[5] We have therefore investigated the Kerr spectra for this compound. These are shown in Fig. 23. Our calculations predict a nice Kerr rotation peak at 3 eV of about $-0.4°$ for RuMnAs. A comparison of the band structure of RuMnAs, which we do not display here, with that of, e.g., PdMnAs, shows that there are hybridized Ru $4d$ bands near E_F (cf. Fig. 22). The Kerr angle peak at the appropriate photon energy position, together with the appropriate T_C and the magnetocrystalline anisotropy, would make RuMnAs an interesting candidate for ultraviolet laser light MO recording applications. Unfortunately, not much is known about other physical properties

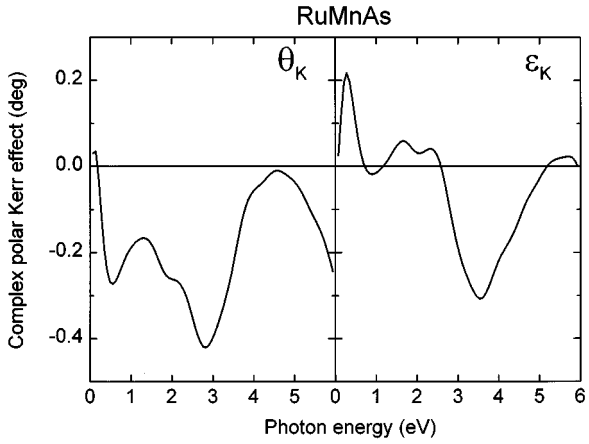

FIG. 23. Predicted Kerr rotation and Kerr ellipticity of RuMnAs.

of RuMnAs. In the related compound RhMnAs, which, in contrast, orders antiferromagnetically, an exotic magnetic behavior (with canted magnetic moments) has been observed.[99–102] It is presently unclear if RuMnAs also exhibits unusual magnetic behavior.[53,92] If this is the case, it would certainly diminish the prospect of applying RuMnAs in MO recording devices.

IV. CONCLUSIONS

We have made a computational investigation of the optical and MO spectra of, first, the half-Heusler compounds NiMnSb, PdMnSb, and PtMnSb, with PtMnSb being the key material of our interest. We have furthermore considered a large number of ternary intermetallic compounds related to PtMnSb. The unusually large MO Kerr angle of PtMnSb, as compared to those of NiMnSb and PdMnSb, can satisfactorily be explained on the basis of *ab initio* band-structure calculations. The differences in the MO Kerr spectra of these three compounds arise straightforwardly as true relativistic band-structure effects. As we have shown explicitly, the half-metallic property of both NiMnSb and PtMnSb does have an indirect influence on the MO Kerr angle, since it leads to a rather small plasma frequency. A small plasma frequency in turn helps to create a minimum in the denominator of Eq. (1). The other quantities that play a role in the ''giant'' Kerr rotation of PtMnSb, are the SO coupling strength of Pt, the large magnetic moment of 4 μ_B on Mn, and the strong hybridization of Mn, Pt, and Sb orbitals.

In the second place we have considered an additional group of other ternary intermetallic compounds in relationship to PtMnSb. We find computationally that none of these related compounds exhibits a MO Kerr effect comparable to that in PtMnSb. This result can be considered to be quite unexpected, because previous computational MO investigations[25,35] revealed unambiguous guidelines for predicting compounds having large Kerr rotations. Although it can be understood how the giant Kerr angle of PtMnSb arises, this illustrates also that PtMnSb does not follow a standard MO behavior. Rather, the aforementioned characteristics of PtMnSb combine fortuitously in a manner which amplifies the Kerr effect.

An interesting off-spin of our investigations is that we predict PtGdBi to be a semiconductor in its ferromagnetic phase. The combination of ferromagnetism and semiconductivity is rarely realized in nature. In the case of PtGdBi the semiconducting property stems from the same origin as the half-metallicity in NiMnSb and PtMnSb, namely, a combined effect of a relatively strong hybridization of the various energy bands and the particular energy band filling.

Finally, we wish to point out that we predict that the As-based ternary intermetallic compounds NiMnAs, PdMnAs, PtMnAs, and RuMnAs will have promising MO spectra for MO recording applications. RuMnAs, particularly, could be a suitable material for MO recording applications, as RuMnAs exhibits a Kerr angle of -0.4 eV at 3-eV photon energy. The MO Kerr spectra of these As-based intermetallics have not been measured as yet. Therefore, we encourage experimental MO investigations of this group of ternary alloys.

Note added in proof. Very recently, a theoretical investigation of the MO Kerr spectra of NiMnSb and PtMnSb were reported by van Ek and Maclaren,[103] who claim that the half-metallic property of these compounds does not play a role for their MO Kerr spectra. Our explicit calculations, however, as outlined in Ref. 24 and in the present work, show that this is not the case.

ACKNOWLEDGMENTS

We are indebted to Professor Katsuaki Sato and Dr. Koki Takanashi for informing us about MO investigations of PtMnSb and related materials. Financial support by the State of Saxony under Contract No. 4-7541.83-MP2/301 is gratefully acknowledged.

*Permanent address: Institute of Metal Physics, Academy of Sciences of Ukraine, 252680 Kiev, Ukraine.

†Author to whom correspondence should be addressed.

[1] P. G. van Engen, K. H. J. Buschow, R. Jongebreur, and M. Erman, Appl. Phys. Lett. **42**, 202 (1983).

[2] P. G. van Engen, K. H. J. Buschow, and M. Erman, J. Magn. Magn. Mater. **30**, 374 (1983).

[3] P. G. van Engen, Ph.D. thesis, Technical University Delft, 1983.

[4] R. A. de Groot, F. M. Mueller, P. G. van Engen, and K. H. J. Buschow, Phys. Rev. Lett. **50**, 2024 (1983).

[5] K. H. J. Buschow, in *Ferromagnetic Materials*, edited by E. P. Wohlfarth and K. H. J. Buschow (North-Holland, Amsterdam, 1988), Vol. 4, p. 588.

[6] J. Schoenes, in *Electronic and Magnetic Properties of Metals and Ceramics*, edited by R. W. Cahn, P. Haasen, and E. J. Kramer, Materials Science and Technology Vol. 3A (Verlag Chemie, Weinheim, 1992), p. 147.

[7] K. E. H. M. Hanssen, P. E. Mijnarends, L. P. L. M. Rabou, and K. H. J. Buschow, Phys. Rev. B **42**, 1533 (1990).

[8] E. Kisker, C. Carbone, C. F. Flipse, and E. F. Wassermann, J. Magn. Magn. Mater. **70**, 21 (1987).

[9] G. L. Bona, F. Meier, M. Taborelli, E. Bucher, and P. H. Schmidt, Solid State Commun. **56**, 391 (1985).

[10] J. S. Moodera and D. M. Mootoo, J. Appl. Phys. **76**, 6101 (1994).

[11] J. F. Bobo, P. R. Johnson, M. Kautzky, F. B. Mancoff, E. Tuncel, R. L. White, and B. M. Clemens, J. Appl. Phys. **81**, 4164 (1997).

[12] R. A. de Groot, F. M. Mueller, P. G. van Engen, and K. H. J. Buschow, J. Appl. Phys. **55**, 2151 (1984).

[13] H. Feil and C. Haas, Phys. Rev. Lett. **58**, 65 (1987).

[14] J. H. Wijngaard, C. Haas, and R. A. de Groot, Phys. Rev. B **40**, 9318 (1989).

[15] P. M. Oppeneer, J. Sticht, and F. Herman, J. Magn. Soc. Jpn. **15**, S1, 73 (1991).

[16] P. M. Oppeneer, T. Maurer, J. Sticht, and J. Kübler, Phys. Rev. B **45**, 10 924 (1992).

[17] S. V. Halilov and R. Feder, Solid State Commun. **88**, 749 (1993).

[18] G. Y. Guo and H. Ebert, Phys. Rev. B **50**, 10 377 (1994).

[19] G. Y. Guo and H. Ebert, Phys. Rev. B **51**, 12 633 (1995).

[20] V. N. Antonov, A. Ya. Perlov, A. P. Shpak, and A. N. Yaresko, J. Magn. Magn. Mater. **146**, 205 (1995).

[21] Xindong Wang, V. P. Antropov, and B. N. Harmon, IEEE Trans. Magn. **30**, 4458 (1994).

[22] E. T. Kulatov, Yu. A. Uspenskii, and S. V. Halilov, Phys. Lett. A **195**, 267 (1994).

[23] Yu. A. Uspenskii, E. T. Kulatov, and S. V. Khalilov, Zh. Éksp. Teor. Fiz. **107**, 1708 (1995) [JETP **80**, 952 (1995)].

[24] P. M. Oppeneer, V. N. Antonov, T. Kraft, H. Eschrig, A. N. Yaresko, and A. Ya. Perlov, Solid State Commun. **94**, 255 (1995).

[25] P. M. Oppeneer and V. N. Antonov, in *Spin-Orbit-Influenced Spectroscopies of Magnetic Solids*, edited by H. Ebert and G. Schütz (Springer, Berlin, 1996), p. 29.

[26] K. J. Kim, T. C. Leung, B. N. Harmon, and D. W. Lynch, J. Phys.: Condens. Matter **6**, 5069 (1994).

[27] T. Gasche, Ph.D. thesis, Uppsala University, 1993.

[28] T. Gasche, M. S. S. Brooks, and B. Johansson, Phys. Rev. B **53**, 296 (1996).

[29] N. Mainkar, D. A. Browne, and J. Callaway, Phys. Rev. B **53**, 3692 (1996).

[30] H. Ebert, Rep. Prog. Phys. **59**, 1665 (1996).

[31] S. Shiomi, A. Ito, and M. Masuda, J. Magn. Soc. Jpn. **11**, S1, 221 (1987).

[32] M. C. Kautzky and B. M. Clemens, Appl. Phys. Lett. **66**, 1279 (1995).

[33] I. Osterloh, P. M. Oppeneer, J. Sticht, and J. Kübler, J. Phys.: Condens. Matter **6**, 285 (1994).

[34] A. Cebollada, D. Weller, J. Sticht, G. R. Harp, R. F. C. Farrow, R. F. Marks, R. Savoy, and J. C. Scott, Phys. Rev. B **50**, 3419 (1994).

[35] P. M. Oppeneer, V. N. Antonov, T. Kraft, H. Eschrig, A. N. Yaresko, and A. Ya. Perlov, J. Phys.: Condens. Matter **8**, 5769 (1996).

[36] W. Reim and J. Schoenes, in *Ferromagnetic Materials*, edited by E. P. Wohlfarth and K. H. J. Buschow (North-Holland, Amsterdam, 1990), Vol. 5, p.133.

[37] J. Kubo, J. Phys. Soc. Jpn. **12**, 570 (1957).

[38] C. S. Wang and J. Callaway, Phys. Rev. B **9**, 4897 (1974).

[39] T. Kraft, P. M. Oppeneer, V. N. Antonov, and H. Eschrig, Phys. Rev. B **52**, 3561 (1995).

[40] P. Hohenberg and W. Kohn, Phys. Rev. **136**, B864 (1964).

[41] W. Kohn and L. Sham, Phys. Rev. **140**, A1133 (1965).

[42] M. E. Rose, *Relativistic Electron Theory* (Wiley, New York, 1961).

[43] R. Feder, F. Rosicky, and B. Ackermann, Z. Phys. B **52**, 31 (1983).

[44] P. Strange, J. B. Staunton, and B. L. Gyorffy, J. Phys. C **17**, 3355 (1984).
[45] H. Eschrig, G. Seifert, and P. Ziesche, Solid State Commun. **56**, 777 (1985).
[46] H. Ebert, Phys. Rev. B **38**, 9390 (1988).
[47] O. K. Andersen, Phys. Rev. B **12**, 3060 (1975).
[48] V. V. Nemoshkalenko, A. E. Krasovskii, V. N. Antonov, Vl. N. Antonov, U. Fleck, H. Wonn, and P. Ziesche, Phys. Status Solidi B **120**, 283 (1983).
[49] U. von Barth and L. A. Hedin, J. Phys. C **5**, 1692 (1972).
[50] A. Santoni and F. J. Himpsel, Phys. Rev. B **43**, 1305 (1991).
[51] G. Lehmann and M. Taut, Phys. Status Solidi B **54**, 469 (1972).
[52] P. Villars and L. D. Calvert, *Pearson's Handbook of Crystallographic Data for Intermetallic Phases* (ASM International, Materials Park, Ohio, 1991).
[53] B. Chenevier, M. Anne, M. Bacmann, D. Fruchart, and P. Chaudouet (unpublished).
[54] P. M. Oppeneer, J. Sticht, T. Maurer, and J. Kübler, Z. Phys. B **88**, 309 (1992).
[55] H. Ebert, H. Freyer, A. Vernes, and G.-Y. Guo, Phys. Rev. B **53**, 7721 (1996).
[56] H. Ebert and G. Schütz, J. Appl. Phys. **69**, 4627 (1991).
[57] S. J. Youn and B. I. Min, Phys. Rev. B **51**, 10 436 (1995).
[58] P. N. Argyres, Phys. Rev. **97**, 334 (1955).
[59] T. Inukai, N. Sugimoto, M. Matsuoka, and K. Ono, Appl. Phys. Lett. **49**, 52 (1986).
[60] K. Takanashi, H. Fujimori, J. Watanabe, M. Shoji, and A. Nagai, Jpn. J. Appl. Phys. **27**, L2351 (1988).
[61] M. Naoe, N. Kitamura, M. Shoji, and A. Nagai, J. Appl. Phys. **63**, 3636 (1988).
[62] K. Takanashi, J. Watanabe, G. Kido, and H. Fujimori, Jpn. J. Appl. Phys. **29**, L306 (1990).
[63] K. Takanashi, K. Sato, J. Watanabe, Y. Sato, and H. Fujimori, Jpn. J. Appl. Phys. **30**, 52 (1991).
[64] K. Sato, H. Ikekame, H. Hongu, M. Fujisawa, K. Takanashi, and H. Fujimori, in *Proceedings of the Sixth International Conference on Ferrites* (Japanese Society of Powder and Powder Metallurgy, Tokyo, 1992), p. 1647.
[65] H. Ikekame, K. Sato, K. Takanashi, and H. Fujimori, Jpn. J. Appl. Phys. **32**, 284 (1993).
[66] P. A. M. van der Heide, W. Baelde, R. A. de Groot, A. R. de Vroomen, P. G. van Engen, and K. H. J. Buschow, J. Phys. F **15**, L75 (1985).
[67] J. Schoenes and W. Reim, Phys. Rev. Lett. **60**, 1988 (1988).
[68] W. Reim, O. E. Hüsser, J. Schoenes, E. Kaldis, and P. Wachter, J. Appl. Phys. **55**, 2155 (1984).
[69] R. Pittini, J. Schoenes, O. Vogt, and P. Wachter, Phys. Rev. Lett. **77**, 944 (1996).
[70] J. Schoenes and R. Pittini, J. Magn. Soc. Jpn. **20**, S1,1 (1996).
[71] T. Kato, H. Kikuzawa, S. Iwata, S. Tsunashima, and S. Uchiyama, J. Magn. Magn. Mater. **140-144**, 713 (1995).
[72] K. W. Wierman and R. D. Kirby, J. Magn. Magn. Mater. **154**, 12 (1996).
[73] E. T. Kulatov, Yu. A. Uspenskii, and S. V. Halilov, J. Magn. Magn. Mater. **163**, 331 (1996).
[74] M. Vergöhl and J. Schoenes, J. Magn. Soc. Jpn. **20**, S1,141 (1996).
[75] P. M. Oppeneer, V. N. Antonov, T. Kraft, H. Eschrig, A. N. Yaresko, and A. Ya. Perlov, J. Appl. Phys. **80**, 1099 (1996).
[76] R. A. de Groot and K. H. J. Buschow, J. Magn. Magn. Mater. **54-57**, 1377 (1986).
[77] M. J. Otto, H. Feil, R. A. M. van Woerden, J. Wijngaard, P. J. van der Valk, C. F. Bruggen, and C. Haas, J. Magn. Magn. Mater. **70**, 33 (1987).
[78] D. Weller, in *Spin-Orbit-Influenced Spectroscopies of Magnetic Solids*, edited by H. Ebert and G. Schütz (Springer, Berlin, 1996), p. 1.
[79] K. H. J. Buschow, J. H. N. van Vucht, P. G. van Engen, D. B. de Mooij, and A. M. van der Kraan, Phys. Status Solidi A **75**, 617 (1983).
[80] G. Q. Di, S. Iwata, S. Tsunashima, and S. Uchiyama, J. Magn. Magn. Mater. **104-107**, 1023 (1992).
[81] G. Q. Di and S. Uchiyama, Phys. Rev. B **53**, 3327 (1996).
[82] R. B. Helmholdt, R. A. de Groot, F. M. Mueller, P. G. van Engen, and K. H. J. Buschow, J. Magn. Magn. Mater. **43**, 249 (1984).
[83] P. C. Canfield, J. D. Thompson, W. P. Beyermann, A. Lacerda, M. F. Hundley, E. Peterson, Z. Fisk, and H. R. Ott, J. Appl. Phys. **70**, 5800 (1991).
[84] Z. Fisk, P. C. Canfield, W. P. Beyermann, J. D. Thompson, M. F. Hundley, H. R. Ott, E. Felder, M. B. Maple, M. A. Lopez de la Torre, P. Visani, and C. L. Seaman, Phys. Rev. Lett. **67**, 3310 (1991).
[85] D. M. Bylander and L. Kleinman, Phys. Rev. B **49**, 1608 (1994).
[86] M. Heinemann and W. M. Temmerman, Phys. Rev. B **49**, 4348 (1994).
[87] I. Tsubokawa, J. Phys. Soc. Jpn. **15**, 1664 (1960).
[88] B. T. Matthias, R. M. Bozorth, and J. H. van Vleck, Phys. Rev. Lett. **7**, 160 (1961).
[89] B. Morisin and N. Narath, J. Chem. Phys. **40**, 1958 (1964).
[90] M. A. Nylund, A. Roger, J. P. Sénateur, and R. Fruchart, J. Solid State Chem. **4**, 115 (1972).
[91] P. Chaudouet, J. Roy Montreuil, J. P. Sénateur, D. Boursier, A. Rouault, and R. Fruchart (unpublished).
[92] T. Harada, T. Kanomata, and T. Kaneko, J. Magn. Magn. Mater. **90&91**, 169 (1990).
[93] H. Brooks, Phys. Rev. **58**, 909 (1940).
[94] G. C. Fletcher, Proc. Phys. Soc. London, Sect. A **67**, 505 (1954).
[95] P. Bruno, Phys. Rev. B **39**, 865 (1989).
[96] K. H. J. Buschow, J. Less-Common Met. **155**, 307 (1989).
[97] R. Carey, D. M. Newman, and B. W. J. Thomas, J. Phys. D **28**, 2207 (1995).
[98] M. Mansuripur, *The Physical Principles of Magneto-Optical Recording* (Cambridge University Press, Cambridge, England, 1995).
[99] B. Chenevier, D. Fruchart, M. Bacmann, J. P. Senateur, P. Chaudouet, and L. Lundgren, Phys. Status Solidi A **84**, 199 (1984).
[100] M. Bacmann, B. Chenevier, D. Fruchart, O. Laborde, and J. L. Soubeyroux, J. Magn. Magn. Mater. **54-57**, 1541 (1986).
[101] T. Kanomata, K. Shirakawa, H. Yasui, and T. Kaneko, J. Magn. Magn. Mater. **68**, 286 (1987).
[102] C. Rillo, J. Bartolomé, M. Bacmann, B. Chenevier, D. Fruchart, and R. Fruchart, J. Magn. Magn. Mater. **104-107**, 1995 (1992).
[103] J. van Ek and J. M. MacLaren, Phys. Rev. B **56**, R2924 (1997).